Draft version April 17, 2021
Typeset using LaTeX **twocolumn** style in AASTeX63

# ASTR 469 Project #2: Analyzing X-ray Data

Jacob Cardinal Tremblay[1]

[1] *West Virginia University, Department of Physics and Astronomy, P.O. Box 6315, Morgantown, WV, USA*

## ABSTRACT

We aim to use Chandra Telescope X-Ray data from PSR J0835-4510, the Vela Pulsar, taken with the Chandra X-Ray Telescope in August 2010 to compute a spectral analysis. The data were separated by soft x-rays and hard x-rays to then analyze the spatial distribution of their ratio which resulted in a value of 0.03. The emission mechanisms of the systems were also analyzed and discussed with the most likely sources being electronic transitions for the soft energies and synchrotron radiation for the hard energies.

*Keywords:* X-rays: stars – pulsars: individual (PSR J0835-4510) – stars: neutron

## 1. INTRODUCTION

X-ray astronomy has been an important part of scientific discovery since it first started in the 1960s. X-ray astronomy has been used in the discovery or study of many hot and high-energy objects, such as x-ray binaries, galaxy clusters, supernovae remnants, material surrounding black holes, and pulsars. It is a distinctive science, as rather than studying photons by collecting large amounts of light and reflecting it towards the detector with a type of mirror or lens, the x-rays must be guided towards the detector in a specific way. This method is required because the refraction index for soft x-rays is given by $\mu \simeq (1-\epsilon)^{0.5}$ (Birney 2006). Because this refractive index is less than 1, and x-rays pass through normal material such as the typical mirrors used in telescopes. The best method then, is to use mirrors, which have low indices to guide the photons towards a detector.

Because X-rays are absorbed the the atmosphere, they can best be detected by space-based telescopes such as the Chandra X-ray Observatory shown in figure 1. This telescope was launched in July of 1999 and was placed in a highly elliptical orbit of around 140,000 km apogee and 10,000 km perigee. The science that this telescope was able to conduct was revolutionary, and combined with the other x-ray observatories which were launched close to that time period, a new era of discovery in high-energy astrophysics was born (Weisskopf et al. 2000). These types of telescopes are perfect to conduct studies of objects which emit in x-ray such as the Vela pulsar, which is the object of interest for this project.

The Vela pulsar, otherwise known as PSR J0835-4510 due to it's position in the sky, was observed with a right ascension (RA) of 08h36m20.70s and a declination (DEC) of -45d10m35.70s with the Chandra telescope. This differs from the now accepted RA and DEC which were measured at radio wavelengths and are of 08h35m20.61149s and -45d10m34.8751s respectively (Dodson et al. 2003). The Vela pulsar is quite interesting, not only is it the brightest pulsar in radio wavelengths, but it also emits at optical, x-ray and gamma-ray wavelengths. By looking at the x-ray data, we are able to compute a specral analysis, which could help other researchers create models for the pulsar which will help determine if the soft component of the radiation originates from surface layers of the neutron star (Pavlov et al. 2001).

**Figure 1.** Illustration of the Chandra X-ray Observatory. Credit: NASA/CXC/NGST

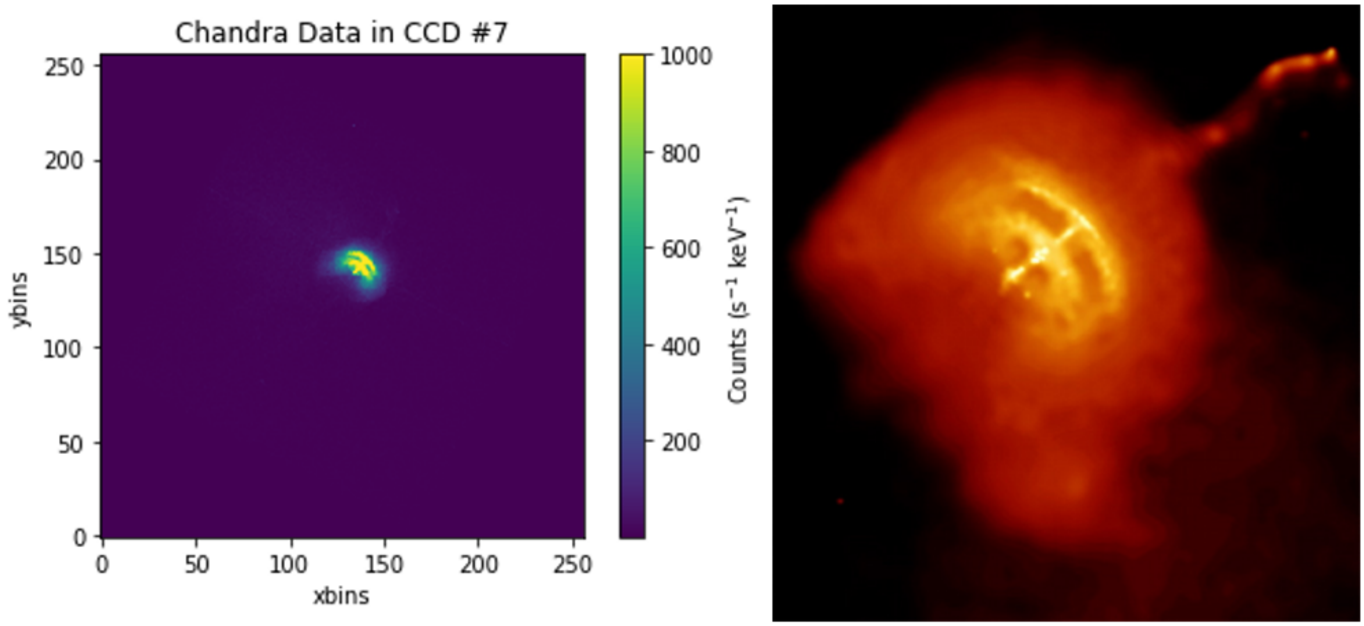


**Figure 2.** Left: Image of the Vela Pulsar created using the Chandra Telescope data for this particular project. Right: Image taken by NASA of the Vela Pulsar using the Chandra Telescope. Image credit: NASA/CXC/PSU/G.Pavlov et al.

## 2. METHODS

### 2.1. *Data*

The initial step in this project was to make sure that there were no temporal problems. Temporal problems could occur from interference such as solar flares, however, after plotting a histogram of the number of counts versus time. The histogram shown in figure 3 demonstrated a relatively constant intensity, and therefore determined that there was no need to exclude certain intervals of time from our data.

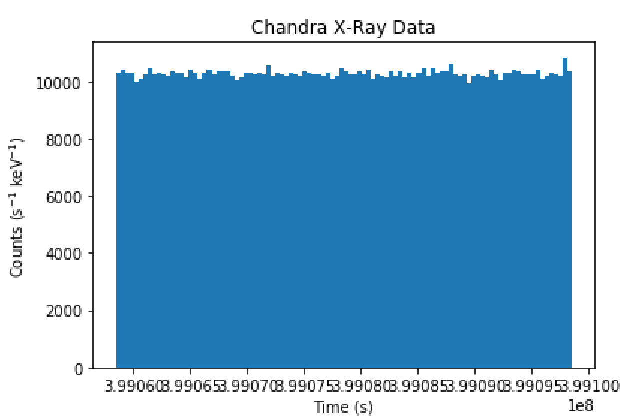


**Figure 3.** Histogram of the Chandra data showing the number of counts versus time.

We did however, only want to include the data from the specific CCD which captured the detection of the Vela pulsar. In order to do so, the x and y events were plotted against each other and we determined the layout of the CCD in order to identify the CCD IDs which would then in turn enable us to locate the CCD with the detection and select only the data from that specific CCD in our observation. We were then able to make a real image. This image was made by plotting a 2D histogram which plotted the values for xbin, ybin and the histogram data. This then produced an image where it was easy to indicate which CCD had made the detection of the Vela pulsar, since it was the CCD which clearly had the highest intensity signal.

It was then determined that CCD number 7 was the CCD which had made the observation, so the data was restricted to only contain information from this CCD. The image was then recreated using only these data and showed a clear observation of the Vela pulsar, with the expected signal shape, as shown in figure 2. Notably, this x-ray image is very similar in shape as other x-ray images taken by NASA.

### 2.2. *Spectral Analysis*

In order to compute a spectral index, it was then necessary to determine which data was a part of the soft x-rays (low energy) and which part of the data was a part of the hard x-rays (high energy). To do this, a histogram plot shown in figure 5 was made which shows the intensity as a function of energy. This plot clearly shows two separate peaks where we are able to determine the concentration of low energy event and high energy event.The low energy seems to show a peak around 1000 eV and the high energy seems to show a peak at 11000

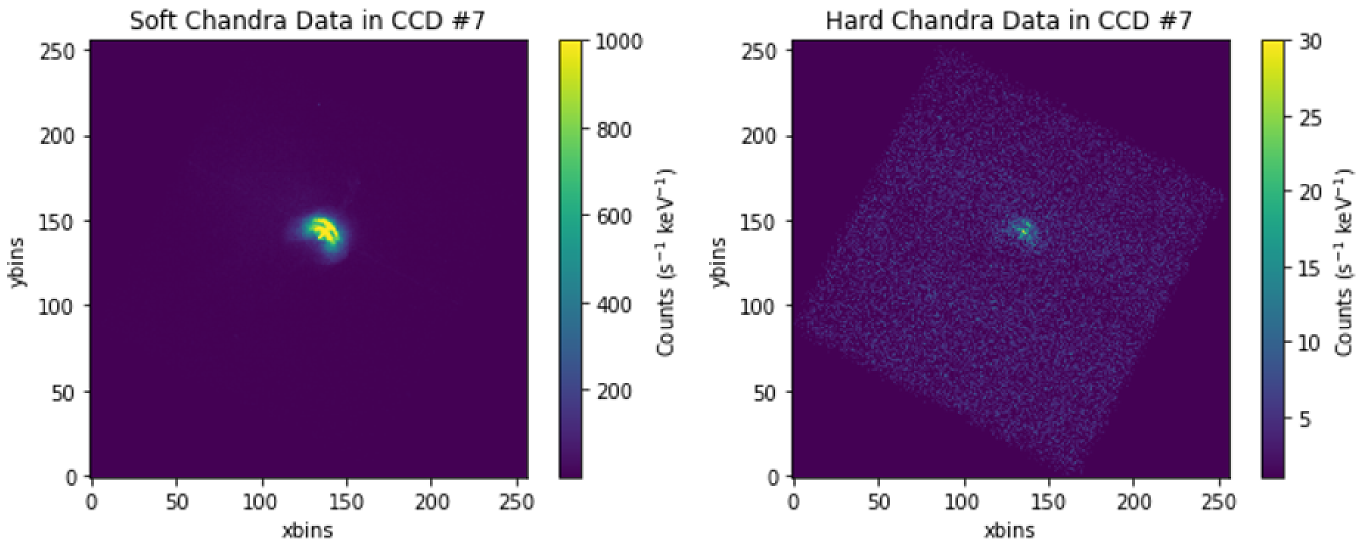


**Figure 4.** Left: Soft x-ray data of the Vela Pulsar. Right: Hard x-ray data of the Vela Pulsar.

eV with the separation between high and low energy occurring around 7000 eV.

We are then able to separate this data. With the delimiter being of 7000 eV, any data below this mark will be considered lower energy, and any data above this mark will be considered higher energy. By doing this, we are able to separate different sources of emission and determine separate sources of emission for the different data. The spectral index may then be calculated by looking at images of the soft and hard emission and then examining the spatial distribution of their ratio.

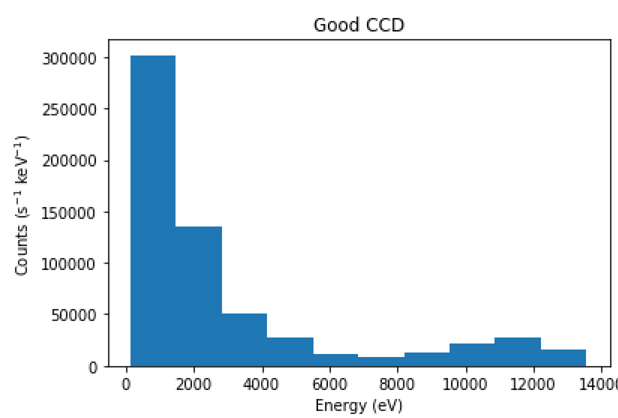


**Figure 5.** Histogram of the energy spectrum.

## 3. RESULTS

By looking at figure 4, we can then estimate the spectral index by examining the spatial distribution of their ratio. Here if we compare the plots in figure 4, we see that the ratio between both is going to be relatively high, since the peak in the soft data is around 1000 counts, whereas the peak in the hard data is around 30. Using these values, we can then calculate the ratio being equal to 0.03, and according to the instructions this ratio is the spectral index $\alpha$.

## 4. DISCUSSION

### 4.1. *Spectral Index*

The result obtained for the spectral index, would imply that although there is a significant peak in the hard energy, almost all of the emission from the source comes from the soft energy. We may also note that the peaks in the soft energy appear throughout the source, including the "double ring feature" whereas the peak in the hard energy appears mostly at a singular point. This can give us a lot of information about the different sources for the different energies.

### 4.2. *Emission Mechanisms*

It is possible to determine the emission mechanisms of both the soft data and the hard data, by understanding the sources of high energy emission. Here it is important to note that there are multiple objects in the Vela system, but the ones which will interact with light will most likely be the pulsar itself and the gas surrounding the pulsar. When looking at the soft data, we see that we detect the light of of an object which appears cloudy and is not a sharp point in space. This, along with the fact that we mostly see this only in the lower energy data, appears to point towards the emission mechanism being from electronic transitions. Radiation from the pulsar (a dense object) is most likely interacting with the gas clouds surrounding the object and causing electronic transitions in the ionized gas.

For the hard energies, there are many effects which could be causing the emission, including a small amount of electronic transition which is powerful enough to emit at such wavelengths. However, for the brightest object in the image, which is a singular point, it is very possible that the Vela pulsar exhibits a strong magnetic field and is emitting synchrotron radiation.

## 5. CONCLUSION

From our results, we conclude that the spectral index of the Vela Pulsar system is of $\alpha = 0.03$. We are also able to determine that the data can be separated into soft energies and hard energies, which come from different emission sources. The soft data most likely coming from electronic transitions, whereas the hard data coming from a mix of synchrotron radiation and electronic transitions.

## 6. ACKNOWLEDGEMENTS

Special thanks to my significant other, Marie Dumaz, the computer scientist who is always there to help me when I run into trouble with my code.

## APPENDIX

*Facilities:* Chandra X-Ray Observatory

*Software:* astropy (Astropy Collaboration et al. 2013; Price-Whelan et al. 2018), numpy (Harris et al. 2020), matplotlib (Hunter 2007), pandas (Wes McKinney 2010; Reback et al. 2021)

## REFERENCES

Astropy Collaboration, Robitaille, T. P., Tollerud, E. J., et al. 2013, Astronomy & Astrophysics, 558, A33, doi: 10.1051/0004-6361/201322068

Birney, D. S. 2006, Observational astronomy / D. Scott Birney, Guillermo Gonzalez, David Oesper., 2nd edn. (Cambridge, UK ;: Cambridge University Press)

Dodson, R., Legge, D., Reynolds, J. E., & McCulloch, P. M. 2003, The Astrophysical Journal, 596, 1137–1141, doi: 10.1086/378089

Harris, C. R., Millman, K. J., van der Walt, S. J., et al. 2020, Nature, 585, 357, doi: 10.1038/s41586-020-2649-2

Hunter, J. D. 2007, Computing in Science & Engineering, 9, 90, doi: 10.1109/MCSE.2007.55

Pavlov, G. G., Zavlin, V. E., Sanwal, D., Burwitz, V., & Garmire, G. P. 2001, The Astrophysical Journal, 552, L129–L133, doi: 10.1086/320342

Price-Whelan, A. M., Sipőcz, B. M., Günther, H. M., et al. 2018, The Astronomical Journal, 156, 123, doi: 10.3847/1538-3881/aabc4f

Reback, J., McKinney, W., Jbrockmendel, et al. 2021, pandas-dev/pandas: Pandas 1.2.1, Zenodo, doi: 10.5281/ZENODO.3509134

Weisskopf, M. C., Tananbaum, H. D., Van Speybroeck, L. P., & O'Dell, S. L. 2000, X-Ray Optics, Instruments, and Missions III, doi: 10.1117/12.391545

Wes McKinney. 2010, in Proceedings of the 9th Python in Science Conference, ed. Stéfan van der Walt & Jarrod Millman, 56 – 61, doi: 10.25080/Majora-92bf1922-00a